

BBA 41112

CIRCULAR DICHROISM AND MAGNETIC CIRCULAR DICHROISM SPECTRA OF CHLOROPHYLLS IN NEMATIC LIQUID CRYSTALS

I. ELECTRIC AND WEAK MAGNETIC FIELD EFFECTS ON THE DICHROISM SPECTRA

DANUTA FRACKOWIAK ^{a,b,*}, DANUTA BAUMAN ^{a,b} and MARTIN J. STILLMAN ^{a,c,*}

^a Centre for Chemical Physics, University of Western Ontario, London, Ontario (Canada), ^b Institute of Physics, Poznan Technical University, Piotrowo 3, 60-965 Poznan (Poland) and ^c Department of Chemistry, University of Western Ontario, London, Ontario (Canada)

(Received April 13th, 1982)

Key words: Chlorophyll; Liquid crystal; Circular dichroism; Magnetic circular dichroism

Dichroism spectra of chlorophyll *a*, chlorophyll *b* and bacteriochlorophyll *a* in various nematic liquid crystals are reported. The initial orientation of chlorophylls in such a sample is determined by the interaction of the aggregate formed from the pigment and the liquid crystal molecules with the electrode surface on the cell windows. Reorientation is carried out by either an electric or magnetic field. The analysis of the circular dichroism spectra obtained from these samples on the basis of the Mueller matrix shows that the intensity is predominantly related to the texture of the sample. Chlorophyll molecules can be aggregated with liquid crystals in two ways: (1) through the chlorin magnesium atom, which results in the liquid crystal chain being almost perpendicular to the porphyrin ring, or (2) attached parallel to the line connecting the first and third pyrrole rings of the chlorin, the chlorin now lying in the plane of the liquid crystal chains. By comparing the dichroism spectra of various chlorophylls in the same liquid crystal we can draw conclusions concerning the preferred type of aggregation, not only with liquid crystals, but also with biological molecules. These liquid crystal systems are models of the orientation effects found for chlorophyll in lamellae. The model studied in this work is much simpler than the lamellar system but it does exhibit several common properties with the latter. Both systems are anisotropic and show much more intense dichroism signals, often of opposite sign, compared with those observed for photosynthetic pigments in isotropic solutions. Dichroism signals of organism fragments are much more complex than those of our model, which can either be related to the occurrence in the organism of several types of pigments or, for a given type of pigment, could be the result of exciton splitting. On the basis of our model it is shown that small changes in the anisotropy of the pigment in the surroundings have a strong influence on the sign and amplitude of the observed circular dichroism signal. Such effects may be responsible for the structure of the dichroism spectra observed for biological samples. Such structures can be partially related to the superposition of the dichroism signal from various 'domains' of chromophore which are different in both pigment arrangement and in the anisotropy of the surroundings of the pigment molecules themselves.

I. Introduction

Analysis of the circular dichroism (CD) spectra of photosynthetic pigments has been widely applied in the elucidation of pigment structures [1], intermolecular interactions [2], determination of the location of pigment in the photosynthetic ap-

* To whom correspondence should be addressed.

Abbreviations: Chl, chlorophyll; BChl, bacteriochlorophyll; DAB, 4-dimethylaminobenzonitril; EBBA, *p*-ethoxybenzylidene-*p*-butylaniline; MBBA, *p*-methoxybenzylidene-*p*-butylaniline; PCB, *p*-pentyl-*p*-cyanobiphenyl. In equations, CB and LB refer to circular and linear birefringence, respectively.

paratus [3–5] and in anisotropic model systems [6,7]. The lamellar system is partially oriented and, therefore, can exhibit several optical effects: linear dichroism (LD), linear birefringence, CD and circular birefringence.

The dichroism spectrum of chlorophylls *in vivo* can be related to the following effects:

- (1) the asymmetry in the chromophore itself, or from the location of chromophore in the complex,
- (2) the helical organization of the lamellar membranes which results in a similar organization of the pigment transition moments, and
- (3) the combination of birefringence of any instrumental elements preceding the sample, as well as any LD of the sample itself [8,9].

The organization of the lamellar system is complicated and not well known. To elucidate the effects of the anisotropic orientation properties of the matrix containing the pigment on the measured ellipticity of chlorophylls, we have constructed a simple anisotropic model of known structure: this is a pigment-doped, liquid crystal cell [10–13].

In the first part of this paper, CD spectra of various chlorophylls, namely, Chl *a*, Chl *b* and BChl *a*, dissolved in three different nematic liquid crystal matrices of known orientation, are reported. In such systems no chlorophyll-chlorophyll aggregation is observed even at high (10^{-3} M) concentrations, which allows us to investigate the interaction between close-lying, uniaxially oriented, but uniformly distributed pigment molecules.

It has been shown previously on the basis of LD measurements [12,13] that in a liquid crystal matrix, the polarization of the chlorophyll absorption spectrum strongly depends on the type of liquid crystal used. The same result is found even when the nonpolarized absorption spectra are almost the same. The specific interactions between solvent and solute molecules can be changed by applying electric and magnetic fields to the measuring cell. A knowledge of the interaction of the chlorophyll with anisotropic surroundings and the perturbation of this interaction by electric and magnetic fields is of value in our understanding of the properties of these pigments in natural lamellar systems and in the interpretation of the dichroism spectra recorded for such systems. Our discus-

sion of the dichroism spectra of anisotropic systems will also be used in the interpretation of the magnetically induced optical activity of similar systems which will be presented in a subsequent paper.

II. Materials and Methods

IIA. Sample preparation

Solutions of chromatographically purified chlorophylls of concentration about 10^{-3} M were prepared in the following liquid crystal solvents: (1) *p*-methoxybenzylidene-*p*-butylaniline (MBBA) + *p*-ethoxybenzylidene-*p*-butylaniline (EBBA); (2) MBBA + EBBA + 4-dimethylaminobenzonitril (DAB); (3) *p*-pentyl-*p*-cyanobiphenyl (PCB).

The first mixture of liquid crystals is characterized by a negative dielectric anisotropy ($\Delta\epsilon < 0$), for the second and third this anisotropy is positive ($\Delta\epsilon > 0$) [14].

The chlorophyll solutions dissolved in the liquid crystal matrices were studied in specially constructed optical cells. Each cell consists of two glass plates on which conducting layers were deposited on the inner surfaces. For such electrodes the 'orienting' silicon oxide (SiO_x) layer was deposited under vacuum using the method of Janing [16]. This procedure enables us to obtain uniform orientation of the liquid crystal molecules within the cell. The liquid crystal molecules are tilted at an angle of about 20° with respect to the electrode surface. Our method of measuring this angle has been given previously [12]. The optically transparent electrodes were assembled for use as a cell with a 20 μm Teflon spacer and then sealed. As a result of a strong interaction between the liquid crystal solvent molecules and the chlorophyll molecules, the pigment molecules orient similarly to the liquid crystal molecules; this is essentially a 'guest-host' effect. This orientation was modified by applying an electric field that ranged from 0 to 10^6 V/m, or a magnetic field that ranged from 0.0 to 5.5 T.

IIB. Description of spectroscopic measurements

Absorption spectra were recorded using a Cary 219 spectrophotometer. A cell filled with pure liquid crystal solvent was used as a reference sample. Dichroism experiments with and without an

external magnet were carried out using either a Jasco J5 CD spectrometer equipped with Sproul SS-20 modifications (at the University of Western Ontario), a Jobin-Yvon Dichrograph Mark III (Paris, France) (in Poland), or with a CD spectrometer constructed by W.R. Browett and M.J. Stillman at The University of Western Ontario. The essential elements of this machine are as follows. A 500 W xenon lamp (Photochemical Research Associates, London, Canada) is used to illuminate the entrance slit of a Cary 14 monochromator. The exit beam is collimated and passed through an MgF_2 Rochon prism (Karl Lambrecht, U.S.A.) and a photoelastic modulator operating close to 50 kHz (Morvue, U.S.A.). A programmed power supply and an Ithaco 391A lock-in amplifier provide two d.c. signals that are plotted simultaneously as the dynode voltage and CD signal, respectively, on a J.J. Lloyd CR 600 two-pen chart recorder (Southampton, U.K.). An Oxford Instruments (Oxford, U.K.) SM2 superconducting magnet provided a variable magnetic field for MCD experiments up to a maximum of 5.5 T.

MCD signal intensities were calibrated by measuring the negative signal at 505 nm observed for aqueous CoSO_4 solutions. In our case, a value for $[\theta]_M$ of $-62.0 \text{ degree} \cdot \text{cm}^2 \cdot \text{dmol}^{-1} \cdot \text{T}^{-1}$ was measured, or in terms of $\Delta\epsilon_M$, $-1.88 \cdot 10^{-2} \text{ l} \cdot \text{mol}^{-1} \cdot \text{cm}^{-1} \cdot \text{T}^{-1}$. CD signal intensities were calibrated by measuring the positive signal at 291 nm of (+)-10-camphorsulfonic acid using $[\theta] = 0.350 \text{ degree} \cdot \text{cm}^2 \cdot \text{dmol}^{-1}$ and the ratio $\theta_{291}^\circ / A_{289\text{nm}} = 2.26$ [16].

Duplicate spectra recorded on each spectrometer were very similar except at the wavelength limits of the Jasco spectrometer ($\lambda > 690 \text{ nm}$) where the slit widths are necessarily large. The data presented here were all recorded on the Cary 14-based spectrometer at the University of West-

ern Ontario, using a fixed slit width of 0.3 mm which results in a spectral band pass of approx. 1.5 nm in the visible region. The dynode voltage trace provides a convenient means of monitoring the single beam absorption spectrum of the sample, and, under the conditions used for these experiments, 1 absorbance unit resulted in a deflection of approx. 2 cm. This proved to be just sufficient to allow us to follow the changes in absorbance as the magnetic field was increased from 0.0 to 5.5 T.

III. Results and Discussion

IIIA. Introduction

The dichroism spectra of Chl *a*, Chl *b* and BChl *a* in various liquid crystal matrices which are shown in Figs. 2–4, were measured with and without the electric field, E , applied to the cell. In addition, the influence of a weak magnetic field was also investigated and the changes in the dichroism spectra are shown in Fig. 5.

A diagram showing the orientation of liquid crystal molecules in electric and magnetic fields for the case of negative and positive liquid crystal dielectric anisotropy is given in Fig. 1. The magnetic anisotropy for all the liquid crystals studied here is positive, therefore, in the case of $\Delta\epsilon < 0$, the result of both E and H is 'antagonistic', whereas for $\Delta\epsilon > 0$, the direction of orientation caused by both fields is the same. Liquid crystal molecules located very close to the window surface maintain their initial tilt angle because of the strong interaction with the orientating layer of SiO_x . As a result, a slightly twisted structure may be formed (Fig. 1). The efficiency of reorientation caused by the applied electric and magnetic fields can be evaluated in the case of mixture of MBBA + EBBA + DAB using the formula [17]:

$$E = \sqrt{4\pi\Delta\xi/\Delta\epsilon H} \quad (1)$$

where $\Delta\epsilon$ and $\Delta\xi$ are the dielectric and magnetic permeability anisotropies, respectively. Taking $\Delta\xi = 1.23 \cdot 10^{-7}$ and $\Delta\epsilon = 0.28$, it was found that the action of an electric field of 1 V/cm corresponds to the action of a magnetic field of 10^{-4} T . In our experiments the application of 1 V to the cell gives $E = 5 \cdot 10^3 \text{ V/cm}$. The largest magnetic field used

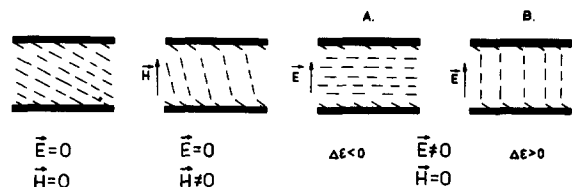


Fig. 1. Scheme for the arrangement of liquid crystal molecules in electric (\vec{E}) and magnetic (\vec{H}) fields.

TABLE I
THE POSITIONS AND HALF BANDWIDTHS, $\Delta\lambda$, OF CHLOROPHYLL ABSORPTION BANDS IN VARIOUS MEDIA

Medium	Position of absorption band, λ (nm)				$\Delta\lambda$ (nm)
	I	II	III	IV	
(A) Chl <i>a</i>					
Diethyl ether	409[19], 410[20]	428[19], 430[20]	578[20]	661[19], 662[20]	8.3[18]
Methanol	—	—	—	664.7[18]	10.4[18]
Benzene	—	—	—	665.6[18]	9.1[18]
Pyridine	—	—	—	671[18]	9.2[18]
Monolayers	420[21], 420[22]	435[21], 440[22]	—	675[19], 680[22]	19[22]
MBBA	420[23]	437[23]	580[23]	671[23]	10[23]
MBBA + EBBA	420[10]	437[10]	580[10]	671[10]	11[10]
MBBA + EBBA + DAB	420	437	580	671	11
LC K15	417[23]	435[23]	—	671[23]	10[23]
PCB	420	437	580	669	10.5
Lecithin	415[24]	437[24]	587[24]	670[24]	—
in vivo	—	438[2]	—	672[23], 683[25]	12.5[2]
(B) Chl <i>b</i>					
Diethyl ether	430[20]	453[20], 452[26]	550[20]	642[20], 642[26]	7.7[26]
MBBA	445[23]	467.5[23]	—	652[21]	—
MBBA + EBBA	440	470	545	662	10
PCB	440	463	540	652	9.5
Lecithin	439[24]	464[24]	548[24]	649[24]	—
in vivo	—	471[2]	—	652[2]	12[2]
(C) BChl <i>a</i>					
Diethyl ether	358[20], 357[27]	391[20], 392[27]	577[20], 573[27]	773[20], 769[27]	17[20]
Methanol	—	365[18]	605[20]	770[20]	26[20]
MBBA + EBBA	—	—	585[12]	788[12]	23.5[12]
PCB	364[12]	396[12]	585[12]	788[12]	23.5[12]
Lecithin	362[24]	385[24]	585[24]	779[24]	—
in vivo	—	376[28]	589[28]	804[28], 880[28]	23[28]

in this work, about 5.5 T, orients the liquid crystal molecules almost perfectly uniaxially and is formally comparable to a 10 V electric field. However, when an electric field is used some ionic processes occur which are totally absent with the magnetic field.

IIIB. Influence of the liquid crystal solvent on the chlorophyll spectrum

Table I summarizes the positions and half bandwidths of the chlorophyll absorption maxima

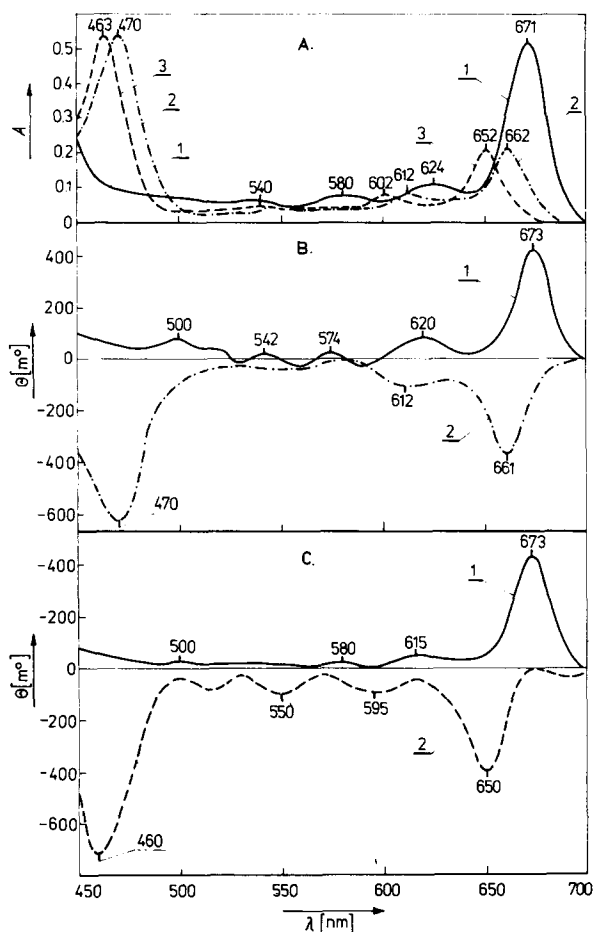


Fig. 2. Absorption and CD (with $\alpha=0^\circ$, for maximum $H=0$ intensity) spectra of Chl *a* and Chl *b* in liquid crystal. (A) Absorption spectra: (1) Chl *a* in MBBA+EBBA ($\Delta\epsilon < 0$); (2) Chl *b* in MBBA+EBBA ($\Delta\epsilon < 0$); (3) Chl *b* in PCB ($\Delta\epsilon > 0$). (B) CD spectra of chlorophylls in liquid crystals with $\Delta\epsilon < 0$: (1) Chl *a* in MBBA+EBBA; (2) Chl *b* in MBBA+EBBA. (C) CD spectra of chlorophylls in liquid crystals with $\Delta\epsilon > 0$: (1) Chl *a* in MBBA+EBBA+DAB; (2) Chl *b* in PCB.

recorded under different conditions: in various solvents, as monolayers, in organisms and in liquid crystals. The positions of the absorption maxima of chlorophyll in liquid crystal solvents more closely resemble those observed for chlorophyll in monolayers and organisms than those of chlorophyll in typical organic solvents. The narrow halfwidths of the absorption bands for the chlorophyll in the liquid crystal solvents (Table I), as well as our previously published data [10,12], indicate that chlorophyll molecules in liquid crystals are dispersed monomerically with a strong chlorophyll-solvent interaction. As a result, the chlorophyll molecules undergo a common reorientation in electric and magnetic fields. With liquid crystals such as MBBA and EBBA, the attachment to the chlorophyll porphyrin ring is parallel to the direc-

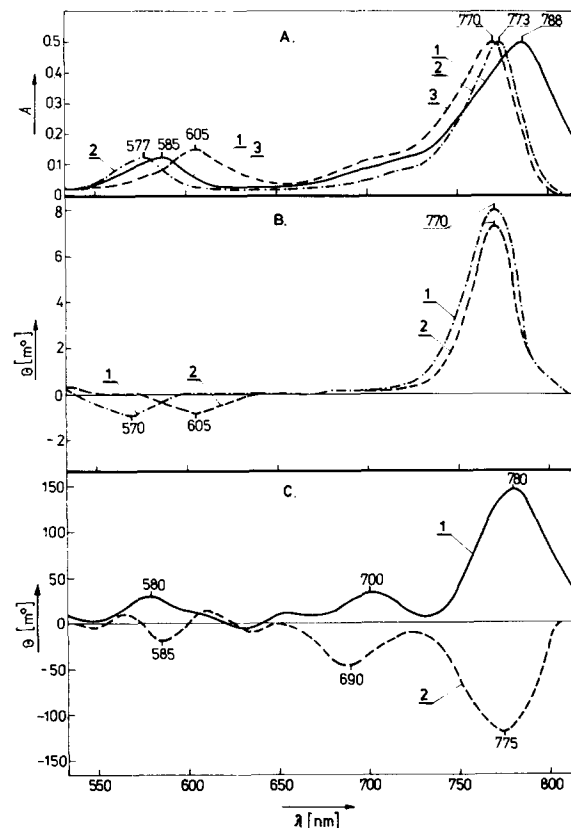


Fig. 3. Absorption and CD ($\alpha=0^\circ$) spectra of BChl *a*. (A) Absorption spectra: (1) BChl *a* in MBBA+EBBA ($\Delta\epsilon < 0$); (2) BChl *a* in acetone; (3) BChl *a* in ethanol. (B) CD spectra: (1) BChl *a* in acetone; (2) BChl *a* in ethanol. (C) CD spectra: (1) BChl *a* in MBBA+EBBA ($\Delta\epsilon < 0$); (2) BChl *a* in PCB ($\Delta\epsilon > 0$).

TABLE II
THE POSITIONS AND SIGNS OF CD MAXIMA OF CHLOROPHYLLS IN VARIOUS MEDIA

Medium	$\lambda(\text{nm})$	Chl <i>a</i>		Chl <i>b</i>		BChl <i>a</i>	
		Chl <i>a</i>		Chl <i>b</i>		BChl <i>a</i>	
Diethyl ether	(+) 400[18], (+) 428[18], (-) 657[18]	(+) 400[18], (+) 428[18], (-) 657[18]	(+) 471[29], (-) 641[29]	(+) 471[29], (-) 641[29]	(-) 571[27], (+) 775[27]	(-) 571[27], (+) 775[27]	(-) 571[27], (+) 775[27]
MBBA + EBBA	(+) 673	(+) 673	(-) 470, (-) 660	(-) 470, (-) 660	(+) 580, (+) 780	(+) 580, (+) 780	(+) 580, (+) 780
MBBA + EBBA + DAB	(+) 673	(+) 673	-	-	-	-	-
PCB	(-) 670	(-) 670	(-) 461, (-) 650	(-) 461, (-) 650	(-) 585, (-) 775	(-) 585, (-) 775	(-) 585, (-) 775
Chloroplasts	(-) 678[4], (+) 690[4]	(-) 678[4], (+) 690[4]	-	-	-	-	-
Ethanol	-	-	-	-	(-) 605, (+) 770	(-) 605, (+) 770	(-) 605, (+) 770
Acetone	-	-	-	-	(-) 570, (+) 770	(-) 570, (+) 770	(-) 570, (+) 770

tion connecting pyrrole rings I and III, whereas for others, for example, PCB, the liquid crystal molecules interact with the central magnesium atom, resulting in an almost perpendicular orientation to the pigment ring [12].

Comparison of the absorption red shifts and the band broadening (Table I) suggests that these liquid crystal molecules belong to the third class of solvent according to the terminology of Seely and Jensen [18]. Therefore, the broadening of the chlorophyll absorption bands is predominantly due to the fluctuating interaction between the transition moments of the solute and the electronic polarization of nearby solvent molecules.

III C. CD spectra

Figs. 2 and 3 show dichroism spectra recorded for Chl *a*, *b* and BChl *a* in liquid crystal cells using the CD spectrometer described earlier. As discussed below, only part of the intensity shown here will arise directly from the phenomenon of CD. Strong absorption by the liquid crystal solvents precludes the recording of the dichroism spectra of chlorophyll in the short-wavelength spectral region, therefore, in Figs. 2 and 3 this part of the spectrum is not shown. Table II summarizes the positions and signs of the dichroism maxima for chlorophylls in chloroplasts, liquid crystals and some organic solvents. Comparing the dichroism spectra in liquid crystals with those in organic solvents (Fig. 3), one can see that the bands in liquid crystals are red shifted and broadened. They are even broader than those of BChl *a* in vivo [4].

Fig. 4 shows the effect on the dichroism intensity of rotating three different liquid crystal thin cells around the optic axis, i.e., around an axis that is perpendicular to the plane of the transparent-electrode windows. The dichroism intensity is monitored at 673 nm in the Chl *a* spectrum in these liquid crystal solvents (Fig. 2B). The angle α is zero for the vertical position of the cell, which is the same as the orientation angle set by the layer of SiO_x on the windows. Thus, the vertical position ($\alpha = 0^\circ$) represents the preferred orientation of the liquid crystal molecules. Fig. 4A shows the intensity changes for Chl *a* in the mixed (MBBA + EBBA + DAB) liquid crystal solvent, and Fig. 4B and C shows traces from two samples of Chl *a* in the same mixed liquid crystal solvent (MBBA +

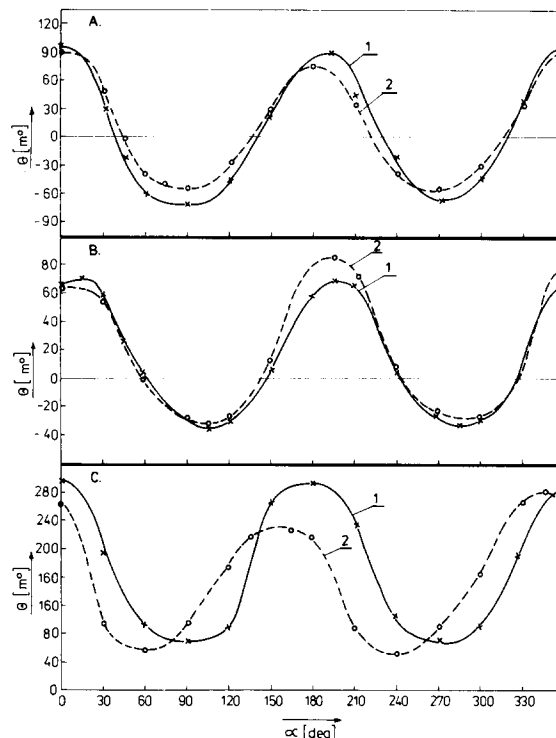


Fig. 4. The change in the CD signal measured at $\lambda = 673$ nm with rotation of a cell filled with Chl *a* in liquid crystal (where α is the angle between initial orientation axis of the liquid crystal and the vertical direction): (1) before application of the voltage; (2) after application of the voltage but with the field off. (A) Chl *a* in MBBA + EBBA + DAB ($\Delta\epsilon > 0$). (B) Chl *a* in MBBA + EBBA, sample 1 ($\Delta\epsilon < 0$). (C) Chl *a* in MBBA + EBBA, sample 2.

EBBA) but in two different cells. The plot of intensity vs. rotation angle, α , displays a cosinusoidal pattern in all three cases (Fig. 4A–C, line 1) as well as after application of the electric field but with E still zero (Fig. 4A–C, line 2). These results can be interpreted as showing that there are two main components in the observed signal at 673 nm. One of these components is harmonically modulated with the cell rotation, the other component is independent of this rotation. The differences between the Chl *a* samples used for Fig. 4B and C is that the initial tilt angle of the liquid crystal in the cell is different, resulting in a significant but constant offset in the cosinusoidal pattern of the 673 nm intensity. Interestingly, the sample used in Fig. 4C exhibited the greatest long-term change in signal following the application of the electric field (Fig. 4C, line 2).

The samples studied in this work exhibit a superposition of at least four effects: LD, CD, linear birefringence and circular birefringence. Each of these phenomena may contribute to the dichroism spectra recorded in this work using the CD spectrometer. LD and linear birefringence are caused by the uniaxial, homogeneous orientation of the pigment molecules; the 'true' CD and the circular birefringence are related to both the molecular asymmetry properties of the chlorophyll molecules and to the helical deformation of the uniaxial arrangement of the chlorophyll chromophores [8,9]. When the measured CD signal is due to LD or linear birefringence properties of the sample located in the modulated light beam of the spectrometer [8,9], this signal will change with α , the angle of the rotation, according to the formulae:

$$LD = LD_{\max} \cdot \cos 2\chi \text{ and } LB = LB_{\max} \cdot \cos 2l$$

where χ and l are the angles formed by pigment and liquid crystal orientation axes to the vertical, respectively. The linear birefringence intensity for the dye will be very small compared with the value of linear birefringence for the liquid crystal.

Before the application of an electric field a regular cosinusoidal feature is observed for θ vs. α (Fig. 4, curve 1) which strongly suggests that the pigment and liquid crystal orientation axes are identical, i.e., $\chi = l$. However, after application of an electric field to the cell, followed by measurement of the CD spectrum with the field off (Fig. 4, curve 2), we find that the relaxation process of chlorophyll-liquid crystal aggregates must be different from that of the liquid crystal molecules alone because the $\theta(\alpha)$ curve is deformed.

The dichroism signal of the oriented samples studied here is of the order 10^9 degree \cdot cm² \cdot dmol⁻¹. This is much higher than that observed for isotropic solutions of chlorophylls, typically approx. 10^5 degree \cdot cm² \cdot dmol⁻¹. Which may be due, in part, to the effects of LD and linear birefringence on the CD signal of the anisotropic sample [8,9] (Fig. 4).

The sign and amplitude of the recorded dichroism signal depend not only on the angle α (Fig. 4) measured in the plane of the cell windows, but also on the angle between the direction of the

oriented transition moments and the direction of propagation of the light, and, additionally, on the degree of orientation of the transition moments. The latter two values may be different for the same pigment in different liquid crystal solvents. An example of this is presented in Fig. 3C, where for the same pigment, BChl *a*, a positive dichroism signal is observed with MBBA + EBBA (curve 1), while a negative signal is observed for PCB (curve 2), both curves being measured at $\alpha = 0^\circ$. It is clear from Fig. 3C that the sign of the dichroism signal in these two cases is opposite. Therefore, by comparing the dichroism spectra of various chlorophylls in the same liquid crystal solvent one can draw conclusions concerning the preferred type of aggregation. For example, Chl *a* and BChl *a* exhibit positive dichroism signals in MBBA + EBBA (Table II, Fig. 2B and C), whereas Chl *b* exhibits a negative signal in both MBBA + EBBA and PCB solvents (Fig. 2B and C), which suggests that its preferred aggregation is through the magnesium atom. It seems likely that the projections on the plane of the cell window of the Q_x and Q_y transition moments of chlorophylls in PCB are similar to one another because the CD spectrum in this solvent is almost independent of α , i.e., θ at $0^\circ = \theta$ at 90° , which results in a flat line in plots similar to those shown in Fig. 4. The extent of any LD intensity on the measured CD signal might well be different in each of the solvents because the intensity depends on the pigment-solvent association.

IIID. Evaluation of the 'true' CD effect

In order to estimate the component of the true CD in the measured dichroism signal, the following formalism described by Jensen et al. [9] was used. The polarized light is described by the Stokes' vector, S , having the following four components: $s_0 = a_x^2 + a_y^2 = I_x + I_y$; $s_1 = 2a_x a_y \cos \delta$; $s_2 = 2a_x a_y \sin \delta$; $s_3 = a_x^2 - a_y^2 = I_x - I_y$, where a_x , a_y and I_x , I_y are amplitudes and intensities of the components of light polarized in the x and y directions, respectively. In general, this means that a sample which cannot be treated as very thin will exhibit dichroism intensity due to:

$$LD = \ln 10 (A_x - A_y) / 2$$

$$LB = 2\pi(n_x - n_y) / \lambda_0$$

$$CD = \ln 10 (A_L - A_R) / 2$$

$$CB = 2\pi(n_L - n_R) / \lambda_0$$

$$LD^1 = \ln 10 (A_{45} - A_{135}) / 2$$

$$LB^1 = 2\pi(n_{45} - n_{135}) / \lambda_0$$

where A_x and A_y represent absorption of plane polarized light along the x - and y -axes, A_L and A_R represent absorption of circularly polarized light, and A_{45} and A_{135} represent absorption when the liquid crystal orientation axes align at either 45 or 135° with respect to the x -axis. The Mueller matrix, M , represents the optical operation on the components of the Stokes vector, S , which describes the incident light, and which yields the components of the final Stokes vector, S_f , according to

$$S_f = MS \quad (2)$$

Taking into account that in each of the CD spectrometers used here the light incident on the sample is modulated (by the Pockel's cells or by the photoelastic modulator), one obtains from the output of modulator [30]:

$$S = \begin{bmatrix} 1 \\ 0 \\ \sin \delta \\ \cos \delta \end{bmatrix} \quad (3)$$

where δ is the instantaneous value of the relative phase shift induced by the modulator for radiation polarized in the direction of its two axes. Taking $\delta = \delta_0 \sin ft$, where f is 2π times the frequency of the modulator oscillation, one can express $\cos \delta$ and $\sin \delta$ in terms of Bessel functions [9].

We experimentally verified that for each sample we used the signal intensity arising from the anisotropic LD was much greater than that from the isotropic CD by rotating the sample about the optical axis. In each case we obtained data similar to those shown in Fig. 4. In addition, because the dichroic absorption at 45 and 135° was found to be close to zero (Fig. 4), the contribution from LD^1 must also be close to zero. Similarly, LB^1 will also vanish. We can, therefore, use a simplified Mueller matrix in the calculation of linear birefringence, LD, circular birefringence and CD, in which

$LD^1 = 0$ and $LB^1 = 0$. The results of this calculation are shown in Table III. When the Mueller matrix is multiplied by the Stokes' vector of the incident light, we obtain values for s which can be compared with the experimental CD signal according to the formula:

$$\tan 2\theta = \frac{s_2}{(s_2^2 + s_3^2)^{1/2}} \quad (4a)$$

and

$$\frac{s_1}{s_3} = \tan 2\alpha \quad (4b)$$

where θ is the ellipticity, α the angle between the long axis of the elliptically polarized light and the x -axis, and $\theta = 33 \Delta A$, where $\Delta A = A_L - A_R$.

The limiting cases were calculated, (1) assuming that the true CD = 0 and that all the measured CD is caused by secondary effects, and (2) assuming that all the measured signal arises from true CD. The calculations were carried out taking δ for the Pockel's cell; in this experimental arrangement there is a greater influence of the modulator on the resulting dichroism. The calculation gives the difference between the two limiting cases of $\Delta\theta = 0.005^\circ$ compared with the measured dichroism signal intensity of approx. 0.400° (Fig. 2). This indicates that the true chlorophyll CD is much smaller than the observed dichroism signal. Therefore, the observed dichroism intensity must be related to the texture of our sample. It follows from the discussion of the origins of Eqns. 2 and 3 and the Mueller matrix (Table III) that for a completely homogeneous, planar orientation of the transition moments in a plane perpendicular to the direction of propagation of the circularly polarized light, the textural dichroism signal that is related to the LD and linear birefringence of the sample must vanish.

It is possible that in the liquid crystal cells studied in this work, a twisted structure is formed as a result of the different orienting forces: (i) the strong interaction between the electrodes and nearby molecules which are oriented by the layer of SiO_x at a tilt angle of about 20° , and (ii) the stronger interaction of the electric or magnetic field on molecules well inside the cell and away from the electrode surfaces. Only a small fraction of one 'pitch' of a helix may be located between

TABLE III

MUELLER MATRIX FOR A MEDIUM WITH LD, LB \gg CD, CB. LD' = LB = 0 [9]

cosh LD	$2(-LD \cdot CB + LB \cdot CD) \cdot [\cosh^2(LD/2) - \cos^2(LB/2)] / (LD^2 + LB^2)$	$(\sinh LD \cdot (LB \cdot CB + LD \cdot CD) + \sin LB \cdot (LB \cdot CD - LD \cdot CB)) / (LD^2 + LB^2)$	$-\sinh LD$
$2(-LB \cdot CD + LD \cdot CB) \cdot [\cosh^2(LD/2) - \cos^2(LB/2)] / (LD^2 + LB^2)$	cos LB	$-\sin LB$	$(\sinh LD \cdot (LB \cdot CD - LD \cdot CB) + \sin LB \cdot (-LB \cdot CB - LD \cdot CD)) / (LD^2 + LB^2)$
$(\sinh LD \cdot (LB \cdot CB + LD \cdot CD) + \sin LB \cdot (LB \cdot CD - LD \cdot CB)) / (LD^2 + LB^2)$	sin LB	cos LB	$2(-LD \cdot CD - LB \cdot CB) \cdot [\cosh^2(LD/2) - \cos^2(LB/2)] / (LD^2 + LB^2)$
$-\sinh LD$	$(\sinh LD \cdot (LD \cdot CB - LB \cdot CD) + \sin LB \cdot (LB \cdot CB + LD \cdot CB)) / (LD^2 + LB^2)$	$2(-LD \cdot CD - LB \cdot CB) \cdot [\cosh^2(LD/2) - \cos^2(LB/2)] / (LD^2 + LB^2)$	cosh LD

the two opposite cell windows, but each application of E or H results in a deformation of this irregular 'helix', and we have found that the cell contents exhibit a memory effect for these deformations for rather a long time. On the basis of the data in Table III and Eqns. 2 and 3, we expect a large contribution to the measured signal intensity from the linear birefringence generated by such a structure.

IIIE. Dependence of the dichroism on applied electric and magnetic fields

The model for the orientation of chlorophyll molecules in a liquid crystal cell proposed in subsection IIIC is in agreement with the dependence

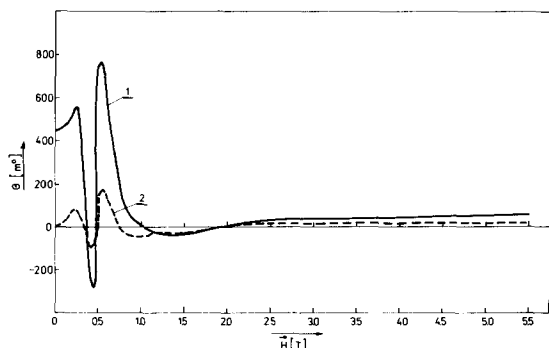


Fig. 5. Ellipticity θ vs. magnetic field: (1) at $\lambda = 673$ nm (near the absorption maximum of Chl a); (2) at $\lambda = 750$ nm (outside the Chl a absorption band); $\alpha = 0^\circ$; the liquid crystal solvent used was MBBA + EBBA.

of the CD signal on an applied magnetic field (Fig. 5). It has been shown by Wooster (quoted by Hartshorne [31]) that a helical arrangement of molecules rotate the plane of polarized light even when the molecules themselves are not optically active. This effect is dependent on both the angle made by the row of molecules arranged in a spiral with a helix axis, and on the relative hands of the helix and the circularly polarized light.

We can calculate the intensity of the dichroism expected for the liquid crystals aligned in our cells by using the equations derived by De Vries [32] for the change in the angle of plane polarized light after passing through cholesteric or twisted nematic liquid crystal layers. Substituting the parameters for the (MBBA + EBBA) liquid crystal mixtures gives a result of 0.150° for the predicted signal. This is quite close to the values observed.

The alignment of liquid crystals is sensitive to the application of magnetic fields. In Fig. 5 we show the change in dichroic intensity as a magnetic field is applied parallel to the optic axis. In curve 1 of Fig. 5 the signal at 670 nm arises from a combination of Chl a and the liquid crystal, whereas curve 2 shows that a similar but far weaker signal is observed for the liquid crystal alone, 750 nm being outside the absorbing region of the Chl a (see Fig. 2). In all the experiments with the magnetic field we observed that there was considerable realignment at lower field strengths (less than 0.7 T) which took some seconds before being completely established, resulting in quite

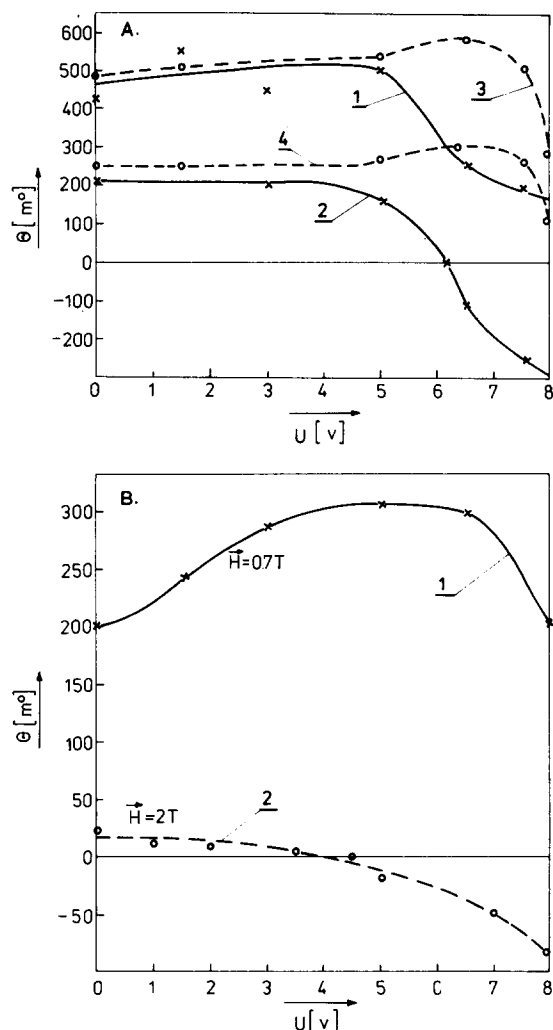


Fig. 6. (A) The dependence of θ (at $\lambda = 673$ nm) on the voltage applied to the cell filled with Chl *a* solution dissolved in: (1) MBBA + EBBA + DAB, $\alpha = 0^\circ$, $\Delta\epsilon > 0$; (2) MBBA + EBBA + DAB, $\alpha = 90^\circ$, $\Delta\epsilon > 0$; (3) MBBA + EBBA, $\alpha = 0^\circ$, $\Delta\epsilon < 0$; (4) MBBA + EBBA, $\alpha = 90^\circ$, $\Delta\epsilon < 0$. (B) θ vs. applied electric potential, in the presence of a weak magnetic field, for Chl *a* in: (1) MBBA + EBBA + DAB, $H = 0.7$ T, $\alpha = 0^\circ$, $\Delta\epsilon > 0$; (2) MBBA + EBBA, $H = 2.0$ T, $\alpha = 0^\circ$, $\Delta\epsilon < 0$.

complex signal patterns that changed significantly with only small (less than $1.0 \cdot 10^{-2}$ T) changes in the magnetic field strength. However, at higher magnetic fields (greater than 1.0 T) we observed only gradual and systematic changes in the dichroic signal (Fig. 5). At these field strengths almost all the liquid crystal and dye molecules are oriented perpendicularly to the plane of the

windows, so that the tilt angle approaches 90° . The measured dichroism is now the MCD that is inherent in the liquid crystal and dye molecules in the absence of any textural effects. As the liquid crystal solvent does not exhibit an MCD spectrum in the absorbing range of the Chl *a* we only observe the weak MCD spectrum of the dye (here Chl *a*, Chl *b* or BChl).

Fig. 6 shows the effect of applying electric and magnetic fields on the intensity measured at 673 nm for Chl *a* in a liquid crystal cell. An increase in the electric field intensity applied without H (Fig. 6A) causes a decrease in θ for liquid crystals with $\Delta\epsilon > 0$, and an increase in θ for liquid crystals with $\Delta\epsilon < 0$, both changes occurring for the same order of magnitude of electric field, i.e. between 6 and 7 V. Above 7.5 V, the signal intensity decreases for both types of liquid crystal. In the first case ($\Delta\epsilon > 0$) the molecules are reoriented, while in the second case ($\Delta\epsilon < 0$) the orientation is at first improved, but then the orientation is perturbed by the formation of so-called 'Williams domains' [17]. For liquid crystals with $\Delta\epsilon > 0$, application of a low, but constant, magnetic field (Fig. 6B), together with an electric field, initially improves the ordering, but at higher electric field values, the ordering becomes perturbed as above. In the case of $\Delta\epsilon < 0$, a stronger magnetic field (2 T) causes a decrease in the initial orientation. An increase in E reorients the molecules, changing the sign of θ .

IV. Comparison between the CD spectra of chlorophylls in liquid crystal model systems and in lamellae

Although these liquid crystal model systems are much simpler than the lamellar system, the liquid crystal model does have several properties in common with the lamellar system. Both systems are anisotropic and exhibit much more intense dichroism signals, often of differently sign, than are observed in the spectra recorded for photosynthetic pigments in isotropic solutions. The CD signals of organism fragments are much more complex than that of our model. This is partially related to the occurrence of several types of pigments and partially as a result of exciton splitting caused by the pigment-protein interactions [4,29].

The liquid crystal model is birefringent, simi-

larly chloroplasts exhibit negative monoaxial double refraction caused, predominantly, by birefringence because this effect decreases and the CD sign changes after the chloroplasts have dried. The CD signal of lamellar fragments is also changed when artificial pigment-protein detergent complexes are denatured [29]. All these results suggest strongly that the CD signal of the natural systems is structure dependent, and the signal intensity arises in part from birefringence and other effects connected with an anisotropic molecular distribution. The origin of the CD signal *in vivo* is usually explained as a result of exciton splitting [29]. Our models do not exhibit strong pigment-pigment interactions and, as a result, do not show any exciton splitting. From other work it has been found that strong anisotropic interactions with the surroundings are the source of the perturbation of LD and polarized fluorescence spectra [12,12]. In the CD spectrum this interaction is shown only by the broadening of the signal. From the analysis of the final Stokes' vector S_r , it follows that the largest influence on the amplitude and sign of the CD spectrum is found when the ordering of the liquid crystal molecules changes, this means that the signal changes are due to linear birefringence.

The CD spectrum observed for natural photosynthetic complexes [29] is composed of two shifted Gaussian curves of opposite sign which arise from exciton splitting of the dimer states. Let us suppose that we can construct a 'mixed' cell with two types of domains from various liquid crystals pigmented by the same type of chlorophyll. As a result of the contributions from the two types of differently oriented domains the observed CD signal will be a superposition of two shifted Gaussian curves of opposite sign. In the biological sample, the anisotropy of the various regions of the chloroplast can be different, this means that the observed CD spectrum will be the sum of the sum of the CD spectra of the chlorophyll molecules located in each of these regions. It is quite likely, then, based on the results of our liquid crystal studies, that both the magnitude and sign of the CD spectrum from these different regions will be different, and, under some circumstances, two or more CD bands may be observed.

Such a model can be useful in the interpretation of the results reported by Pearlstein and Hemenger

[33] which show that BChl-protein complexes possess CD structure which cannot be explained simply by exciton splitting. These authors proposed two possible explanations: (1) that in BChl *a* the lowest energy transition moment is 'x-polarized', opposite to the more usual y-polarization; (2) that there is some systematic error in the protein structural model.

We now show a third possibility, the CD signal splitting can be related to the optical anisotropy of the surroundings of the pigment together with the anisotropic location of the pigment itself, both of which can change the CD spectrum expected for the various types of BChl molecules. Even in macroscopically unoriented samples, such an effect can be observed as the result of photoselection by the measuring light beam which gives a signal for the average orientation of the transition moments of the various types of pigments.

Acknowledgements

The authors wish to thank Dr. H. Manikowski for very helpful discussions and the Centre for Chemical Physics at the University of Western Ontario for a Visiting Fellowship (to D.F.) and for travel assistance (to D.B.). M.J.S. is a member of Centre for Chemical Physics at the University of Western Ontario. We gratefully acknowledge financial support under project No. MR 11.7 coordinated by the Institute of Ecology of the Polish Academy of Sciences (to D.F.), from the Natural Sciences and Engineering Research Council of Canada (to M.J.S.) and from the Academic Development Fund at the University of Western Ontario for equipment (to M.J.S.).

References

- 1 Ciardelli, F. and Salvadori, P. (1973) *Fundamental Aspects and Recent Developments in Optical Rotatory and Circular Dichroism*, Heyden and Son Ltd., London
- 2 Van Metter, R. (1977) *Biochim. Biophys. Acta* 462, 642-658
- 3 Gregory, R.P.F. and Raps, S. (1974) *Biochem. J.* 142, 193-201
- 4 Gregory, R.P.F. (1975) *Biochem. J.* 148, 487-497
- 5 Demeter, S., Mustardy, L., Machowicz, E. and Gregory, R.P.F. (1976) *Biochem. J.* 156, 469-472
- 6 Norden, B. (1978) *Appl. Spectrosc. Rev.* 14, 157-248

- 7 Kuball, H.G., Karstens, T. and Schönhefer, A. (1976) *Chem. Phys.* 12, 1–12
- 8 Davidsson, Å., Norden, B. and Seth, S. (1980) *Chem. Phys. Lett.* 70, 313–316
- 9 Jensen, H.P., Schellman J.A. and Troxell, T. (1978) *Appl. Spectrosc.* 32, 192–200
- 10 Frackowiak, D., Bauman, D., Manikowski, H. and Martyński, T. (1977) *Biophys. Chem.* 6, 369–377
- 11 Frackowiak, D. (1978) *Photochem. Photobiol.* 28, 377–382
- 12 Bauman, D. and Wróbel, D. (1980) *Biophys. Chem.* 12, 83–91
- 13 Frackowiak, D. (1978) *Acta Phys. Polon.* A54, 757–760
- 14 Priestley, E.B. (1975) in *Introduction to Liquid Crystals* (Priestley, E.B., Wojtowicz, P.J. and Sheng, P., eds.), pp. 1–13/203–217, Plenum Press, New York
- 15 Janning, J.L. (1972) *Appl. Phys. Lett.* 21, 173–174
- 16 Chen, G.C. and Yang, J.T. (1977) *Anal. Lett.* 10, 1195–1207
- 17 De Gennes, P.G. (1975) *The Physics of Liquid Crystals*, Clarendon Press, Oxford
- 18 Seely, G.R. and Jensen, R.G. (1965) *Spectrochim. Acta* 21, 1835–1840
- 19 Houssier, C. and Sauer, K. (1970) *J. Am. Chem. Soc.* 92, 779–791
- 20 Goedheer, J.C. (1966) in *The Chlorophylls* (Vernon, L.P. and Seely, G.R., eds.), pp. 147–184, Academic Press, New York
- 21 Jacobs, E.E., Holt, A.S. and Rabinowitch, E. (1954) *J. Chem. Phys.* 22, 142–143
- 22 Bellamy, W.D., Gainer, G.L. and Tweet, A.G. (1963) *J. Chem. Phys.* 39, 2528–2538
- 23 Journeaux, R. and Viovy, R. (1978) *Photochem. Photobiol.* 28, 243–248
- 24 Hoff, A.J. (1974) *Photochem. Photobiol.* 19, 51–57
- 25 Clayton, K. (1966) in *The Chlorophylls* (Vernon, L.P. and Seely, G.R., eds.), pp. 610–641, Academic Press, New York
- 26 Bauer, R.K., Szalay, L. and Tombacz, E. (1972) *Biophys. J.* L2, 731–745
- 27 Philipson, K.D. and Sauer, K. (1972) *Biochemistry* 11, 1880–1885
- 28 Brody, M. and Linschitz, H. (1961) *Science* 133, 705–706
- 29 Gregory, R.P.F. (1977) in *Primary Processes of Photosynthesis* (Barber, J., ed.), pp. 466–492, Elsevier/North-Holland, Amsterdam
- 30 Brecht, S., Demeter, A. and Faludig, D. (1982) *Photochem. Photobiophys.* 3, 153–157
- 31 Hartshorne, N.H., (1974) in *Liquid Crystals and Plastic Crystals* (Gray, G.W. and Winsor, P.A., eds.), pp. 24–61, Ellis Harwood, Chichester.
- 32 De Vries, A. (1951) *Acta Crystallogr.* 4, 219–226
- 33 Pearlstein, R.M. and Hemenger, R.P. (1978) *Proc. Natl. Acad. Sci. U.S.A.* 75, 4920–4924